LA-5654

C.3

UC-41
Reporting Date: June 1974
Issued: October 1974

CIC-14 REPORT COLLECTION
REPRODUCTION
COPY

Particle Size Distribution of Fragments from Depleted Uranium Penetrators Fired Against Armor Plate Targets

by

W. C. Hanson
J. C. Elder
H. J. Ettinger
L. W. Hantel
J. W. Owens

LOS ALAMOS NATIONAL LABORATORY
3 9338 00377 3180

los alamos
scientific laboratory
of the University of California
LOS ALAMOS, NEW MEXICO 87544

UNITED STATES
ATOMIC ENERGY COMMISSION
CONTRACT W-7405-ENG. 36

Completion report of Task 2, Project Order 4-670A-133 to Reimbursable Activities Branch, USAEC, Albuquerque, NM, for USAF Armament Laboratory, Eglin Air Force Base, FL.

Printed in the United States of America. Available from
National Technical Information Service
U.S. Department of Commerce
5285 Port Royal Road
Springfield, Virginia 22151
Price: Printed Copy $4.00 Microfiche $1.45

PARTICLE SIZE DISTRIBUTION OF FRAGMENTS FROM DEPLETED URANIUM PENETRATORS FIRED AGAINST ARMOR PLATE TARGETS

by

W. C. Hanson, J. C. Elder, H. J. Ettinger, L. W. Hantel, and J. W. Owens

LOS ALAMOS NATL. LAB. LIBS.
3 9338 00377 3180

ABSTRACT

This report describes particle size distributions of fragments of depleted uranium (DU) penetrators fired against armor plate targets. The experiments were conducted at the request of the U. S. Air Force Armament Laboratory, Eglin Air Force Base, Florida, to provide information needed to evaluate the environmental impact of such munitions. These data will serve as input to a model for evaluation of human exposures to aerosols generated by the pyrophoric action of DU penetrators.

I. AIRBORNE URANIUM PARTICLES

A. Introduction

The particle size characteristics of a toxic material are an essential consideration in an environmental impact statement because of their effect on the material's mobility in air, water, or soil and on its probability of inhalation and lung deposition. This study was designed to define the aerodynamic characteristics of aerosol produced when a depleted uranium (DU) projectile penetrates a thick section of armor plate.

Samples of the aerosol produced following armor penetration by depleted U-0.75 wt% Ti penetrators were obtained from enclosures in front of and behind the armor plate. The sample air was recirculated, creating minor air flow and local turbulence within the enclosures. This sampling configuration was considered to approximate an open-air environment with very slight wind dispersion. Containing all of the aerosol within these steel enclosures, rather than allowing dispersion into an unlimited volume of air, probably promoted coagulation or agglomeration of small particles by increasing the particle concentration. This experimental constraint might increase the aerosol median diameter with time as coagulation proceeds, and might also decrease the median diameter after an additional time owing to fallout of the larger agglomerates that form continuously. The particle size characteristics and concentration are difficult terms to define precisely because of these conflicting effects and because they fluctuate continuously as a function of time.

The sampling arrangement consisted of sample chambers upstream (ahead of) and downstream from (behind) the armor plate target. The aerosols produced in each chamber were sampled for size analysis separately, assuming a possible significant difference in aerosol characteristics upstream and downstream from the armor plate. Investigation of the reasons for these differences was considered beyond the scope of this study. All airborne material produced was assumed to be pyrophoric and to have been completely oxidized to UO_2 within the first minute and to U_3O_8 before sample analysis. Fumes consisting of chains of small, roughly spherical particles were expected, because they have been observed in other studies.[1]

Analyses for titanium and uranium were performed separately. Uranium analysis by fluorimetry and titanium analysis by atomic absorption revealed the mass of each element in nine size fractions.

B. Experimental Apparatus and Techniques

1. Particle Size Separation by Andersen Impactor. The eight-stage Andersen impactor was selected as the sampler for particle size analysis.[2] This device is simple and easy to operate in the field, and it provides size separation over a wide range of particle diameters. Size separation is based on inertial properties of the aerosol, and the impactor's calibration is well documented.[3,4] Particles entering an impactor stage are accelerated through multiple jets and directed toward an impaction surface. Larger particles with enough inertia leave the flow path and strike the impaction surface. Smaller particles with less inertia continue on to succeeding stages in which smaller jets and higher velocities cause them to deposit eventually according to their aerodynamic size. Particles small enough to clear all the impactor stages are collected by a backup, 47-mm-diam, Millipore type AA membrane filter (MF) that, in effect, becomes a ninth collection stage and provides nearly absolute collection of the smallest particles.

The eight impaction stages provided effective cutoff diameters (ECD) at 11, 7, 4.7, 3.3, 2.1, 1.1, 0.65, and 0.43 μm. ECD has been used to describe the size range of particles that remain on a given stage of the impactor and to define the aerodynamic particle size collected with 50% efficiency on that stage.[5] Because of the actual cutoff characteristics, some particles larger than the ECD pass a given stage and some particles smaller than the ECD are collected on that stage. However, in describing an aerosol size distribution using impactor data, it is convenient and accurate enough to assume step function cutoffs at the ECDs.[5] Particle size distributions may then be described in cumulative form (cumulative percent less than a given aerodynamic size). If the particles' aerodynamic diameters are log normally distributed (as very often happens naturally), the parameters of the particle size distribution are the mass median aerodynamic diameter (mmad) and the geometric standard deviation (σ_g). An mmad is a statistical diameter above or below which half the total mass of the distribution occurs. σ_g is an index of dispersity, ranging from $\sigma_g = 1$ when all particles are the same size to $\sigma_g = 5$ or more when there is a very broad size spectrum.

The samples were collected on Millipore AA membrane filter medium (3-1/8 in. diam) covering each impactor plate. This surface provided a convenient sample carrier and reduced the particle rebound problems that are associated with some aerosols when individual particles strike bare stainless steel impaction plates.

2. Sampling Enclosures. Steel chambers of moderate volume contained the large fragments and prevented dispersal of airborne particles whose sedimentation time was reasonably long. A 0.27-m^3 stainless steel box with 0.635-cm-thick walls was mounted on the back of a heavy steel plate used to keep the target rigid during penetration. The armor plate target was mounted on the front of the steel plate and was enclosed in a standard 55-gal (0.25-m^3) steel drum through which the projectile passed. Figures 1 and 2 show the backstop and chambers.

Two Andersen impactors with backup MFs were connected to the exit chamber to sample from 2.54-cm-diam ports in each side wall approximately 15 cm above the floor and 15 cm behind the backstop plate. The sample air flow was returned to the chamber through two ports in the roof near the rear wall. This recirculation provided an air flow pattern from top rear to bottom front and maintained uniform atmospheric pressure within the chamber. Two samplers drawing air from the entrance chamber pulled fresh air into the chamber through the hole made to permit unobstructed passage of the penetrator to the armor plate. This hole was large enough to admit 0.0566 m^3/min (2ft.^{3}/min) of air without developing negative pressure in the front chamber. Although there was also a large hole between the front and rear chambers, equilized pressure prevented gross interchange of aerosol between them. These sampling enclosures excluded large amounts of sand particles or other extraneous material, limiting the sample constituents to oxidized uranium, titanium from the penetrator and armor plate, and steel from the armor plate and chambers.

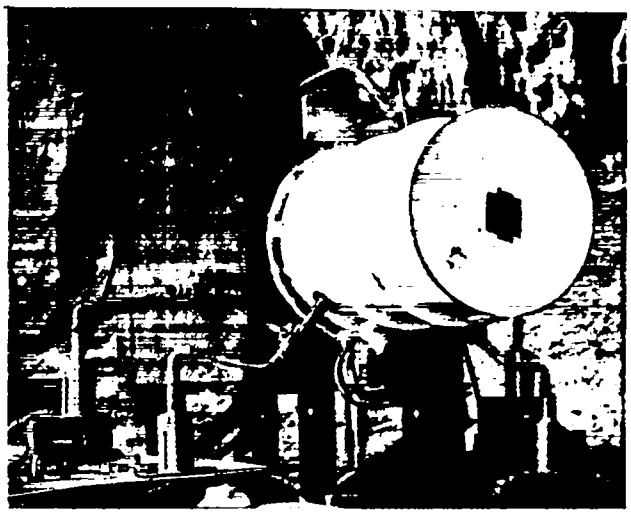

Fig. 1.
Sampling apparatus (entrance chamber at near end).

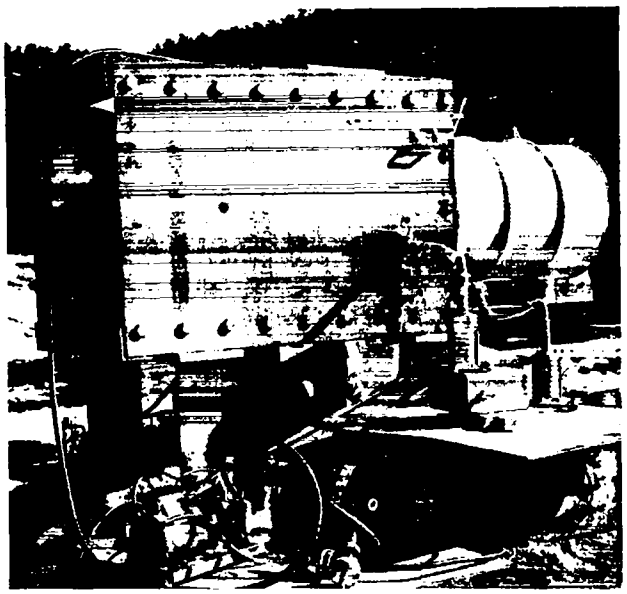

Fig. 2.
Sampling apparatus (exit chamber inside backstop).

Samples were considered valid when the projectile penetrated the armor plate but not the rear chamber, and when there was reasonable deposition on the impactor stages without visible deposition on the impactor walls owing to overloading of the stages.

3. Fluorophotometric Determination of Uranium. The fluorophotometric method is based on the intense yellow-green fluorescence (principal line at 555 nm) produced by traces of uranium fused in sodium fluoride.[6] It is sensitive to about 5×10^{-11} g of uranium per 0.25 g of sodium fluoride, with a precision of $\pm 10\%$. The samples of uranium-titanium aerosol deposited on cellulose acetate filters were ashed in concentrated HCl and H_2SO_4, dried, and then brought to the desired volume with water. An aliquot of the sample solution was placed in a platinum dish and dried. After an initial fusion step, about 0.25 g of sodium fluoride was added to the dish and heated until completely fused. The dishes were cooled and placed in the fluorophotometer where the fluorescence of the fused disk was read. The mass of uranium per sample was determined from an appropriate standard curve. Several blanks were processed identically to provide a zero for the fluorophotometer. Most of the samples taken were extremely high in uranium mass, and required a 100:1 dilution before analysis. Three aliquots were taken from each sample solution, and the average of these three analyses is reported.

4. Determination of Titanium by Atomic Absorption. The atomic absorption technique is based on the ability of atoms of every element to absorb radiation in very narrow wavelength bands that are different for each element.[7] To be able to absorb, the atoms must be chemically unbound and in their minimum energy state, a condition generally achieved by vaporizing the sample in a flame.

The radiation source is generally a hollow-cathode lamp whose cathode is made of the element being determined and which emits the line spectrum of that element. The sample absorbs only at a certain line (called the resonance line). After passing the flame containing the sample vapor, the resonance line is diminished by the sample absorption, whereas all other lines are unaffected. The other lines are removed by a monochromator that is tuned to select a band of wavelengths around the resonance line and to reject all others. The photodetector then sees only the diminished-resonance line. Atomic absorption obeys Beer's Law: concentration of the element in the sample is proportional to the absorbance (log transmittance^{-1}).

The sample solutions were prepared for analysis using the procedures described for uranium. The aqueous solution was aspirated at a known rate into the N_2O-acetylene gas stream that supplied the flame. The concentration scale had previously been calibrated by analyzing known samples. The method threshold was estimated to be 4 μg with a precision of ± 4 μg.

5. Calculation of Sedimentation Velocity. To illustrate the importance of particle fallout, we calculated the sedimentation velocity of particles coinciding in size with the ECD of each stage of the Andersen impactor by using the Stokes formula and the Cunningham slip correction:[8,9]

$$V_s = \frac{2r^2 g \rho}{9 \eta} \left(1 + \frac{A\lambda}{r}\right) , \qquad (1)$$

where

V_s is sedimentation velocity (cm s^{-1}),
r is particle physical radius (cm),
g is acceleration due to gravity (981 cm s^{-2}),
ρ is particle density (11.0 g cm^{-3}),
η is viscosity of air (183×10^{-6} g s^{-1} cm^{-1} at 20°C),
A is Millikan's constant (0.90 estimated),
λ is the mean free path of gas molecules ($\sim 8.5 \times 10^{-6}$ cm at 20°C and 58 cm Hg).

These calculated values are summarized in Table I.

TABLE I

SEDIMENTATION VELOCITIES AT IMPACTOR EFFECTIVE CUTOFF DIAMETERS

Stage No.	ECD (μm)	Phys. Radius (μm)	Sed. Vel. (cm s^{-1})	Time to Fall 70 cm[a] (s)
0	11.0	1.6	0.335	210
1	7.0	1.0	0.126	555
2	4.7	0.71	0.055	1273
3	3.3	0.48	0.025	2800
4	2.1	0.28	0.0088	8000
5	1.1	0.12	0.0016	4 4000
6	0.65	---	---	---
7	0.43	---	---	---

[a]Sample chamber height.

C. Results and Discussion

We fired five shots to obtain particle size characteristics for one set of operating conditions. All data from the first shot and half the samples from Shots 2 and 3 were lost because of overloading of the impactor plates. Sampling times were subsequently shortened to 10 s to reduce these loadings. Although samples this small were necessary for loading, they were undesirable in terms of sampling error. A rigorous estimate of sampling errors is beyond the scope of the requested study, but typical errors include: (1) ±5% flow measurement variations that result in stage cutoff inaccuracies of 0.5 μm for larger particles and 0.05 μm for smaller particles, (2) variations in delay times between armor penetration and initiation of sampling which cause differences in initial aerosol agglomeration and losses owing to sedimentation, and (3) variations in penetration conditions which affect the aerosol mass and number concentration which, in turn, can significantly change agglomeration rates.

The results of the uranium particle study are summarized in Table II in terms of the measured mmad and σ_g. These values are limited to uranium, because titanium quantities were barely above the analytical method's detection threshold. The few titanium analyses above this threshold indicated a titanium:uranium ratio reasonably consistent with the alloy ratio of the penetrator, the mean and standard deviation of 34 positive observations being 0.011 ± 0.006. The particle size distribution derived from each set of impactor samples satisfied an arbitrary criterion for log normality; that is, no data point deviated from a least squares best fit line by more than 10%. The assumption of log normality permitted graphical determination of mmad from the 50% intercept of a plot of cumulative percent less than a stated diameter vs diameter on log probability paper. The geometric standard deviation (σ_g), an index of dispersity obtained from the same plot, is the ratio of diameter at the 84% intercept to diameter at the 50% intercept.

Table II shows a fairly wide distribution of particle sizes for any of the uranium aerosols, as described by σ_gs of 1.7 to 3.3, mmads of 2.1 to 4.2 μm, and an aerosol in the exit chamber somewhat larger in mmad than that in the entrance chamber. The last observation may be a result of greater agglomeration owing to the higher particle concentration in the exit chamber. As noted later, the larger mmads associated with Shots 4 and 5 were accompanied by higher mass concentration (>1 g m^{-3} in the exit chamber).

Agreement in mmad between the impactors sampling each chamber was good, with the possible exception of Impactors 3 and 4 on Shot 4. Impactor 3 results appear questionable in the shot, when compared to the results of Shot 5. Direct comparison of shot results may be tenuous owing to undefinable variations in test conditions, the major variation probably being the behavior of the projectile as it penetrated the armor plate.

Uranium particle size distributions in the entrance and exit chambers are presented in Figs. 3 and 4 as least squares best fit lines on log probability graphs.

TABLE II

URANIUM PARTICLE SIZE CHARACTERISTICS

	Entrance Chamber						Exit Chamber					
	Impactor 1			Impactor 2			Impactor 3			Impactor 4		
Shot	mmad[a]	σ_g	Time[b]	mmad	σ_g	Time[b]	mmad	σ_g	Time[b]	mmad	σ_g	Time[b]
2	2.8	2.4	2	3.0	2.1	2.2	---	---	---	---	---	---
3	---	---	---	---	---	---	2.8	3.1	4	2.4	3.0	5
4	2.1	3.3	2	2.6	2.4	2	2.6	2.5	4	4.2	1.8	5.5
5	3.4	1.8	2	3.3	2.0	2	4.2	1.8	4	3.9	1.7	7

[a]Mass median aerodynamic diameter in microns.

[b]Sample starting time, minutes after shot.

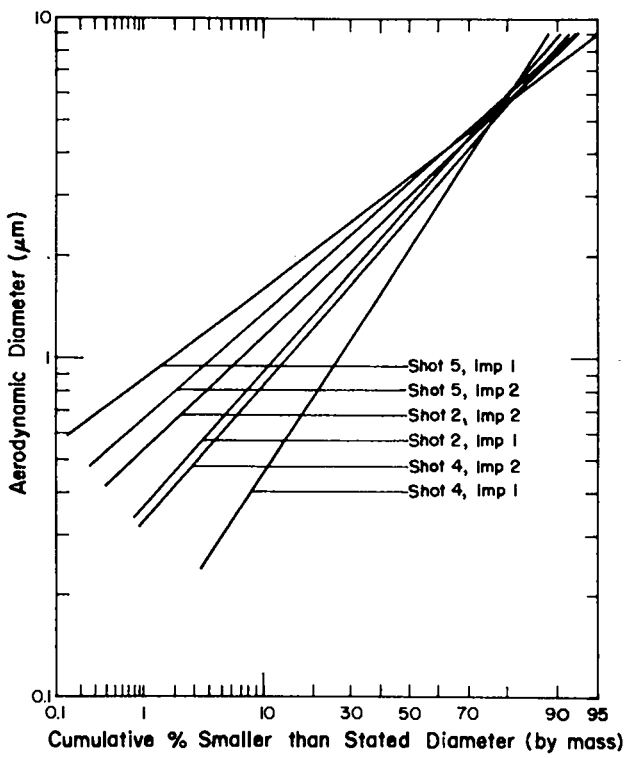

Fig. 3.
Least squares best fit of particle size distribution (entrance chamber).

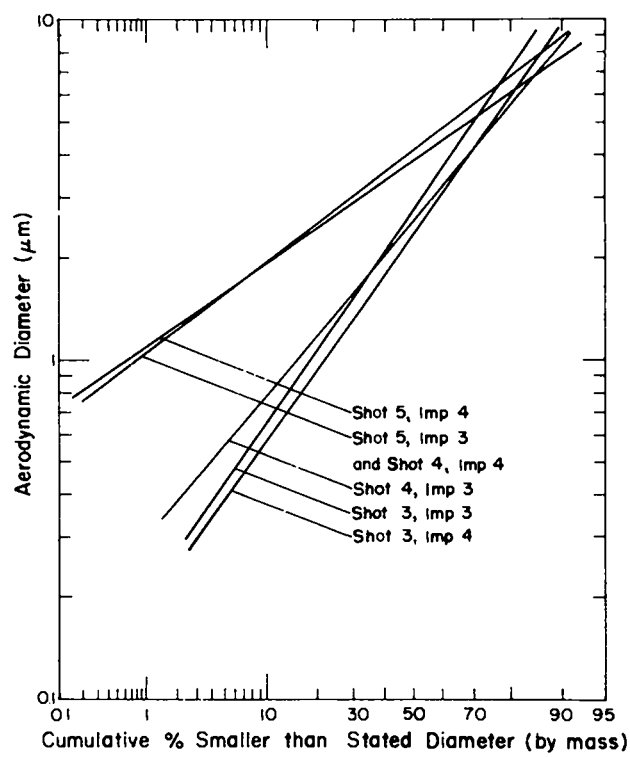

Fig. 4.
Least squares best fit of particle size distribution (exit chamber).

This graphical display of the results listed in Table II indicates more clearly the similarity of size distributions in both chambers and allows easier visualization of the limits within which given size characteristics might be expected to occur.

Mass concentrations, summarized in Table III, were higher by roughly a factor of 3 in the exit chamber. These concentrations, listed as uranium rather than UO_2, are extremely high compared to the threshold limit value for natural ^{238}U for the 40-h/wk occupational exposure[10] of 0.2 mg m^{-3}. The

TABLE III

URANIUM MASS CONCENTRATIONS IN THE SAMPLE CHAMBERS (mg m^{-3})

	Entrance Chamber		Exit Chamber	
Shot	Imp. 1	Imp. 2	Imp. 3	Imp. 4
2	69	95	---	---
3	---	---	1014	529
4	243	323	873	1209
5	636	501	1664	1126

discrepancy of almost a factor of 10 between Shots 2 and 5, Impactor 1, also is unexplained.

The estimated analytical error in mass concentrations in Table III is ±5.5%, based on ±2.5% error in the sum of nine impactor stage deposits and ±5% error in sample volume. Wall losses and handling losses were not included in this estimate as they were probably small. Variations owing to nonuniformity of the aerosol within the chambers were not quantified, but they probably introduced the largest potential error.

Particulate deposition in the lungs is a function of particle size.[11] Respirable dust is that part of the inhaled dust which is deposited in the nonciliated parts of the lung. The concept of respirable fraction as a function of particle size of toxic dust which may lead to lung disease has been established in several standards[10,12]. The mass fraction of the aerosol which is "respirable" can be determined from either standard as a function of mmad and σ_g.[13] The fraction of penetrator mass constituting the respirable aerosol can be estimated roughly by calculating airborne mass in each chamber (mass concentration times chamber volume), determining the respirable fraction from the American Conference of Governmental Industrial Hygienists (ACGIH) curve based on the measured aerosol size characteristics, and summing the mass of respirable aerosol in both chambers. These results are listed in Table IV. The higher of the two respirable mass values from each shot might be summed in the interest of conservatism. Note that these high respirable mass values indicate a need to evaluate the potential inhalation hazard to personnel exposed frequently in test areas.

We considered the possible effects of agglomeration on mass concentration and median particle size theoretically to rule out gross changes occurring during the time lapse between samples (2 to 7 min after the shot). To illustrate the effect of agglomeration, we calculated the particle number concentrations of several size distributions with size characteristics (mmad and σ_g) at both extremes using the Smoluchowski relationship[8]

$$\frac{dn}{dt} = -Kn^2 \quad , \tag{2}$$

which integrates to

$$n = \frac{n_0}{1 + Kn_0 t} \quad , \tag{3}$$

where

n is the particle number concentration at time t,
n_0 is the initial particle concentration,
K is the agglomeration constant $m^3 s^{-1}$.

TABLE IV

MASS OF RESPIRABLE AEROSOL

Shot	Imp.	Chamber	Resp. Fraction	Mass (mg)	Resp. Mass (mg)
4	1	Entr	0.62	60.8	37.7
4	2	Entr	0.61	80.8	49.2
4	3	Exit	0.61	236	144
4	4	Exit	0.42	326	137
5	1	Entr	0.50	159	79.5
5	2	Entr	0.50	125	62.6
5	3	Exit	0.42	449	189
5	4	Exit	0.42	304	128

The agglomeration constant K for a monodisperse aerosol ($\sigma_g = 1$) must be calculated using the Cunningham mobility formula[8]

$$K = \frac{4}{3}\frac{kT}{\eta}\left(1 + \frac{A\lambda}{r}\right), \qquad (4)$$

where

k is Boltzmann's constant (1.380×10^{-16} erg K^{-1}),
T is absolute temperature (293 K),
η is air viscosity (186×10^{-6} g $s^{-1}cm^{-1}$ at 293 K),
A is Millikan's constant (0.90 estimated),
λ is mean free path of gas molecules (8.5×10^{-6}cm),
r is particle radius (cm).

Obtaining a representative particle radius for use in this expression entails conversion of the mmad obtained from impactor data (Table II) to mass median diameter (mmd) using Stokes' equation,[8] conversion of the mmd to count median radius (cmr) using the Hatch and Choate equations,[14] and conversion of the cmr to the arithmetic mean radius ($\bar{r}$) of the distribution, also by using the the Hatch and Choate equations. Because Eq. (4) applies only to a monodisperse aerosol ($\sigma_g = 1$), we calculated a correction factor for polydispersity (ϕ).[8] The results of these calculations, the agglomeration constant for a polydisperse aerosol (K_p), are listed in Table V. Dividing total particle volume by the volume of the particle of average volume provided the particle number concentration during the time of sampling. We calculated concentration halving time t_H, the time required for half the initial number of particles to disappear, by solving Eq. (3) for t and setting $n = n_o/2$. Table V indicates the large effect of particle size characteristics, particularly σ_g, on the rate of particle number change. The aerosols with low median diameter and high σ_g contain very large numbers of particles and exhibit very short halving times, even though the corresponding mass concentration may be low. Because the rate of particle number change varies as the square of particle concentration during the agglomeration process, very rapid changes occur until the aerosol "ages" to much lower number concentrations. To illustrate this point, Fig. 5 shows number concentration as a function of time for an aerosol with agglomeration constant $K = 10^{-14} m^3 s^{-1}$ and initial number concentration $N_0 = 10^{16} m^{-3}$. This aerosol's size characteristics are similar to those of the first two aerosols in Table V. The major change in the aerosol occurs in the first 20 to 30 s. Major particle size

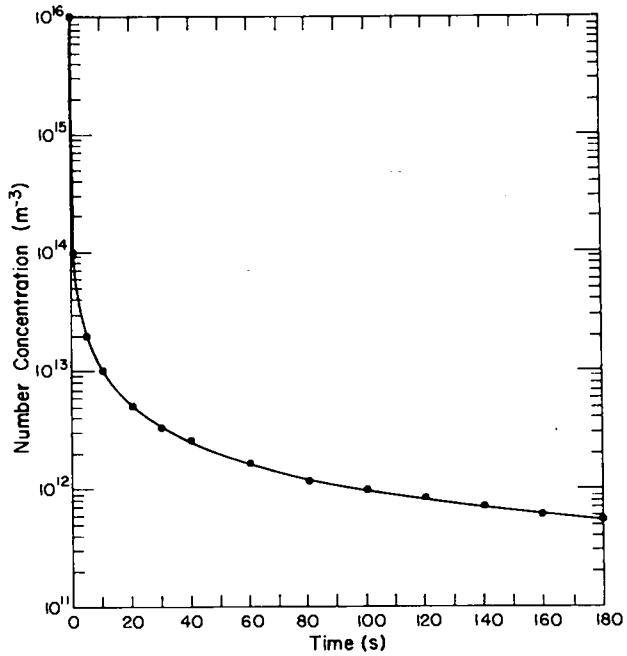

Fig. 5.
Removal curve for a reference aerosol with agglomeration constant $K = 10^{-14} m^3 s^{-1}$.

TABLE V

PARTICLE NUMBER CONCENTRATIONS AND HALVING TIMES FOR TYPICAL AEROSOLS

Shot	Imp.	mmad (μm)	σ_g	mmd (μm)	cmd (μm)	$\bar{r}$ (μm)	$K \times 10^{15}$ (m^3s^{-1})	ϕ	$K_p \times 10^{15}$ (m^3s^{-1})	$\bar{D}_v$ (μm)	Particle Number (m^{-3})	^tH(s)
4	1	2.1	3.3	0.56	0.0078	0.0080	3.08	8.99	27.7	0.066	1.48×10^{14}	0.24
3	3	2.8	3.1	0.77	0.017	0.016	1.70	1.81	3.07	0.11	1.22×10^{14}	2.67
5	1	3.4	1.8	0.92	0.32	0.19	0.405	1.31	0.530	0.55	6.75×10^{11}	2800
5	3	4.2	1.8	1.17	0.41	0.25	0.380	1.30	0.492	0.70	8.60×10^{11}	2360

growth and σ_g reduction occurs during this period. It is unlikely that major mass concentration reduction is caused by particle fallout during this period, because particle diameters near 0.01 μm (Table V) would have to grow to >1.6 μm (Table I) to give short sedimentation times in the chamber.

At t = 2 min, N has decreased to 8.3×10^{11} m^{-3}; at t = 4 min, N = $4.2 \times 10^{11} m^{-3}$. The number-halving time is roughly 2 min at this point and it becomes longer as t increases. Although quantitative agglomeration effects on particle median size and mass concentration are still unknown, we can conclude that all rapid changes had ceased by the time of the first sampling and that the reported results represent the aerosols of greatest interest in an environmental impact study.

We located some potentially relevant comparative data in several articles. Machine shop operations produce small chips that burn and produce UO_2 aerosols whose mmads range from 0.4 to 3.9 μm.[15] Dry-milling produces the larger (2.3- to 3.7-μm) aerosols, whereas machining with a coolant apparently removes most of the large particles and produces aerosols at the smaller end of the range. Ball-milled UO_2 produces aerosols in a fairly narrow range of sizes (mmads 1.1 to 1.4 μm) and geometric standard deviations (σ_gs 2.0 to 2.8).[16] Metallic uranium heated in air at 1200°C produced agglomerated particles with 1- to 2-μm microscopic diameter or approximately 3- to 6-μm aerodynamic diameter.[1] These articles indicate that a wide range of particle sizes can be expected from violent disruption or heating of solid pieces of uranium metal and that a very high fraction of the particles produced will be in the respirable range. The present study serves to confirm these points.

D. Summary

The aerosol produced when a depleted uranium projectile penetrated a thick piece of armor plate has been sampled using eight-stage Andersen impactors to determine its particle size characteristics. These size characteristics, expressed as mass median aerodynamic diameter and geometric standard deviation, are a valuable contribution to any environmental impact statement concerning the mobility of UO_2 particles in air and their probability of inhalation.

Five shots were fired to gain particle size information, but only four gave useful data. The aerosols formed by pyrophoric action on small uranium particles were contained in steel chambers ahead of and behind the armor plate. Analysis of samples from two impactors drawing from each chamber provided the mass of uranium and titanium deposit in nine size classification intervals (0.43 to 11 μm). Summation of mass in these intervals also provided an approximate mass concentration in the chamber.

Titanium mass analysis indicated uranium:titanium proportions consistent with those of the penetrator alloy. Particle size characteristics based on uranium mass analysis (not UO_2) show generally respirable (2.1- to 4.2-μm) mmads, large (1.7 to 3.3) σ_gs, and an aerosol with somewhat larger mmad in the exit chamber, which may be attributable to extensive agglomeration in the very high mass concentration of particles found in the exit chamber. The average mass concentration of uranium from Shot 5, which produced the most aerosol, was 570 mg/m^3 in the entrance chamber and 1400 mg/m^3 in the exit chamber. The mass fraction of the aerosol considered respirable according to the ACGIH standard ranged from 42 to 62%.

II. LARGER URANIUM FRAGMENTS

A. Introduction

This section of the report analyzes larger uranium-titanium-steel armor plate fragments than those sampled by the Andersen impactors. The Andersen impactor data principally concerned aerosol particles that are important in defining the inhalation hazard near targets. The particle size composition of larger fragments is also of concern in estimating the total environmental impact of depleted uranium (DU) penetrators. Scenarios have been developed for military application of DU munitions in specific areas where DU deposition on landscapes must be estimated to quantify the toxicological aspects of DU.

B. Methods

We collected larger penetrator fragments separately from the 0.25-m^3 entrance and 0.27-m^3 exit chambers after collecting aerosol samples and dismantling the target following each shot. The walls were completely brushed, and all fragments in each chamber were collected in plastic vials for transport to the laboratory. These fragments were then processed through a U. S. Standard Sieve Series mounted on a Ro-Tap Testing Sieve Shaker and shaken for 10 min. This process yielded size fractions of < 53-, 53- to 105-, 105- to 500-, 500- to 2000-, 2000- to 5660-, and >5660-μm fragments. The fractions were then weighed and individually dissolved in aqua regia (1 part concentrated HNO_3 to 3 parts concentrated HCl, including one volume of H_2O).

Fluorometric determination of the uranium was unacceptable because of the high uranium concentrations and the quenching effect of the uranium ion in the samples. Therefore, we used a modified Procedure 384 for the uranium determination.[17] This is a thiocyanate method that uses a spectrophotometer to read the yellow complex. Two percent accuracy is claimed for the procedure, and all of the standards and spiked samples were within this range. However, there was considerable variation in subsampling of the two largest size fractions from both entrance and exit chambers of Shots 4 and 5, because of the inhomogeneous distribution of uranium within any one size fraction.

C. Results

The five experimental shots were made with DU penetrators of average 271.8-g weight containing 0.63 to 0.70% titanium. They were fired into vertical armor plate targets at 0° obliquity at velocities that varied by only 2% from maximum to minimum. Reconstruction of the DU mass balance for the shots (Table VI) showed that most of any penetrator was recovered in the rear chamber. The percent of any penetrator recovered in the entrance chamber varied over a hundredfold compared to only sixfold variation in the exit chamber. The greatest discrepancy in entrance chamber contents was between Shots 2 and 5, which confirms the aerosol particle results. Maximum recovery in both chambers occurred on Shot 5, whose velocity was about 10 m/s less than that of the previous three shots. There is no immediate explanation of why Shot 5 maintained its integrity during penetration rather than fragmenting as much as other penetrators, particularly Shot 4.

The size distribution of fragments and their uranium content is summarized in Table VII. There was consistently greater variability in uranium content and in fragment sizes between 105 and 5660 μm in entrance chamber samples than in exit chamber samples. This variability was presumably caused by highly variable backscatter upon impact and by large pieces (up to 60 g) of unfragmented penetrators and armor plate that were often recovered in the exit chamber. Several 105- to 5660-μm fragments were composed of agglomerated smaller particles that were partially fused. The coefficients of variation (CV) for this range of particle sizes were often near 1.0, compared to 0.5 in the >5660-μm, and 0.8 in the <53-μm, range.

Replicate analyses of the two larger fragment size fractions (2000 to 5660 and >5600 μm) from both entrance and exit chambers on Shots 4 and 5 indicated uranium content CVs of 13% in the smaller fragments and 100% in the larger. There was much greater variation (150 vs 50%) in subsamples from the exit chamber than in subsamples from the entrance chamber, probably because of inclusion of large fragments of pure steel or pure DU in the exit chamber.

About 80% of the total sample weight and uranium content usually occurred in the large fragment fraction from the exit chamber, except for Shot 4 which fragmented into the next two smaller size fractions. Distribution of uranium content of the large fragment

TABLE VI

URANIUM MASS BALANCE IN ENTRANCE AND EXIT CHAMBERS
(Percent of Penetrator Weight)

Shot	Entrance Chamber	Exit Chamber	Total	Remarks
1	0.7	---	0.7	Did not penetrate.
2	0.3	41.7	42.0	
3	1.2	26.8	28.0	
4	1.8	8.7	10.5	
5	31.4	53.7	85.1	Lowest velocity.
Means (2-5)	8.7	32.7	41.4	
S.D. (2-5)	15.2	26.6	31.9	

TABLE VII

DISTRIBUTION OF SAMPLE WEIGHT AND URANIUM CONTENT BY FRAGMENT SIZE

Chamber	Total Sample Weight (g)	Fragment Size Range (μm) <53 % wt[a]	<53 % U[b]	53-105 % wt	53-105 % U	105-500 % wt	105-500 % U	500-2000 % wt	500-2000 % U	2000-5660 % wt	2000-5660 % U	>5660 % wt	>5660 % U	Percent U in Total Recovered Material
1-Entrance	142.6	0.11	0.76	0.23	2.19	2.53	14.13	6.90	36.41	14.56	16.43	75.66	30.08	1.26
2-Entrance	140.1	0.16	1.07	0.19	0.40	2.48	16.91	7.01	31.36	16.73	10.60	73.42	39.66	0.54
3-Entrance	135.0	0.10	0.48	0.12	0.22	1.89	3.45	5.94	16.24	16.91	3.29	75.04	76.32	2.52
4-Entrance	161.7	0.19	1.35	0.40	2.03	2.43	6.54	5.74	13.40	18.88	37.91	72.36	38.77	3.10
5-Entrance	155.1	0.36	0.11	0.47	0.07	2.55	0.28	5.99	0.51	12.98	1.21	77.66	97.72	54.93
Means (2-5)	148.0	0.20	0.75	0.30	0.68	2.34	6.80	6.17	15.38	16.38	13.25	74.62	63.11	15.28
S.D.	12.5	0.11	0.56	0.17	0.91	0.30	7.21	0.57	12.66	2.46	16.92	2.31	28.95	26.48
2-Exit	207.0	0.59	0.21	0.50	0.22	2.85	0.59	3.08	0.86	8.79	11.70	84.19	86.42	54.91
3-Exit	173.0	0.24	0.32	0.25	0.30	1.76	0.90	4.30	8.34	13.29	19.91	80.15	70.23	42.09
4-Exit	164.8	0.35	1.57	0.30	1.37	1.15	4.27	4.48	23.30	12.52	62.36	81.20	7.13	14.13
5-Exit	238.7	0.92	0.98	0.36	0.33	0.95	1.00	3.88	4.61	11.34	14.40	82.54	78.68	61.08
Means (2-5)	195.9	0.52	0.77	0.35	0.56	1.68	1.69	3.94	9.28	11.48	27.09	82.02	60.66	43.10
S.D.	33.9	0.30	0.63	0.11	0.54	0.85	1.73	0.62	9.83	14.67	23.76	39.32	36.29	20.74

[a]Percent of total sample weight.

[b]Percent of total uranium recovered.

NOTE: To calculate the grams of uranium in any particular size fraction, multiply total sample weight (g) times fraction of uranium in total sample times fraction of uranium in size fraction. For example, in 1-Entrance 53- to 105-μm fraction: (142.6) (0.0126) (0.0219) = 0.039 g of uranium in (142.6) (0.0023) = 0.328 g total sample wt.

fraction in the entrance chamber was highly variable from shot to shot, whereas the sample weight fraction was consistently near 75% for the same series of shots.

D. Discussion

These results suggest that penetration by DU munitions is a complex mechanism that generates fragments whose armor plate and DU compositions are highly variable. This situation was probably complicated by the confined nature of the experiment, which promoted fusion and agglomeration of particles. This experiment was typical of most in that it posed nearly as many questions as it answered. For instance, samples from the entrance chamber of Shot 1 (which did not penetrate the armor plate) showed nearly the same fragment size distribution and uranium composition as shots that completely penetrated the target. Shot 5 yielded unusually high uranium concentrations in the largest fragment sizes and unusually low uranium concentrations in the smaller fragments in the entrance chamber, even though the mass distribution was generally similar to those of the other three shots.

Comparison of the larger fragments with the aerosol samples showed similar shifts in sample composition. The unusual difference between results from impactors 3 and 4 on Shot 4 correlated with a shift in uranium concentration from the >5660-μm size fraction toward above average concentrations in the 500- to 2000- and 2000- to 5660-μm fractions. The low production of aerosol particles by Shot 2 also correlated with a uranium concentration shift toward fragments in the 105- to 500- and 500- to 2000-μm ranges. As noted above, Shot 5 exhibited unusually high uranium concentration in the >5660-μm fragments compared to the other shots; this concentration correlated positively with the higher generation of aerosol (Fig. 6).

E. Summary and Conclusions

Fragments produced by four DU penetrators fired into armor plate targets showed a higher concentration of large particles in the exit chamber than in the entrance chamber. Compounded samples of the six size fractions from the exit chamber contained nearly three times the uranium found in similar aggregate samples from the entrance chamber. An average of 41% of the penetrator uranium mass was accounted for in the size fractions. This mass was distributed in a 1:4 ratio between entrance and exit chambers, indicating that much of the DU penetrator pierced the armor plate unfragmented.

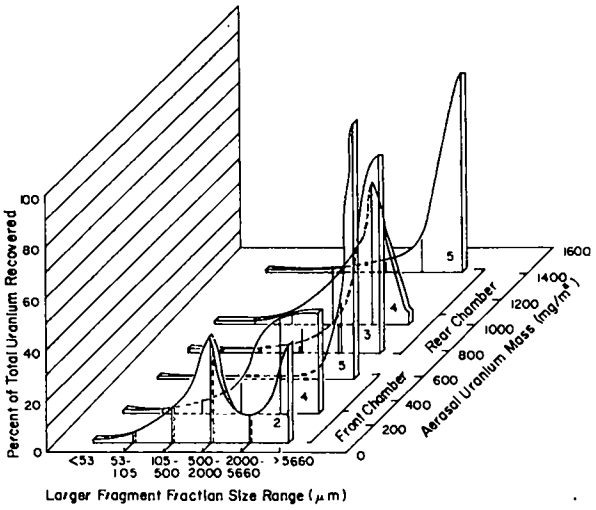

Fig. 6.
Aerosol vs larger fragment components of uranium.

Aerosol data collected by impactors were positively correlated with larger fragment sizes. Production of uranium aerosol was low when a greater uranium concentration was observed in fragments in the 105- to 500- and 500- to 2000-μm ranges, compared to high aerosol production when the greatest uranium concentration occurred in >5660-μm fragments.

The relatively small (0.27- and 0.25-m^3) volumes of the collection chambers apparently caused fusion and agglomeration of particles. This constraint on the data is not serious, but it should be borne in mind in applying the results to field situations. We conclude that these results provide a reasonable estimate of a potential hazard to personnel frequently exposed in test areas or in combat.

REFERENCES

1. G. W. Parker, G. E. Creek, and W. J. Martin, "Fuel Element Decomposition Products," Seventh AEC Air Cleaning Conference, Upton, NY, Oct. 10-12, 1961, TID-7627, pp. 263-283.

2. A. A. Andersen, "A Sampler for Respiratory Health Hazard Assessment," Am. Ind. Hyg. Assoc. J. **27**, 160 (1966).

3. J. P. Flesch, D. H. Norris, and A. E. Nugent, Jr., "Calibrating Particulate Air Samplers with Monodisperse Aerosols: Application to the Andersen Cascade Impactor," Am. Ind. Hyg. Assoc. J. **28**, 507 (Nov. - Dec., 1967).

4. K. R. May, "Calibration of a Modified Andersen Bacterial Aerosol Sampler," Appl. Microbiol. **12**, 37 (1964).

5. T. T. Mercer, "On the Calibration of Cascade Impactors," Ann. Occup. Hyg. **6**, 1 (1963).

6. M. F. Milligan, "Analytical Procedures of the Industrial Hygiene Group," Los Alamos Scientific Laboratory report LA-1858, 2nd Ed. (Sept. 1958).

7. W. J. Price, *Analytical Atomic Absorption Spectometry* (Heyden & Son, London, 1972) Ch. 2, p. 8.

8. N. A. Fuchs, *The Mechanics of Aerosols* (The MacMillan Company, New York, 1964), pp. 23, 290, and 296.

9. E. Cunningham, "On the Velocity of Steady Fall of Spherical Particles Through a Fluid Medium," Proc. Roy. Soc. **A-83**, 357-365 (1910).

10. American Conference of Governmental Industrial Hygienists, "Threshold Limit Values for Chemical Substances and Physical Agents in the Workroom Environment: 1973."

11. T. F. Hatch and P. Gross, *Pulmonary Deposition and Retention of Inhaled Aerosols* (Academic Press, New York, 1964), Ch. 8, p. 147.

12. BMRC, "Recommendations of the British Medical Research Council Panels Relating to Selective Sampling," in *Inhaled Particles and Vapors* (Pergamon Press, London, 1961), p. 475.

13 O. R. Moss and H. J. Ettinger, "Respirable Dust Characteristics of Polydisperse Aerosols, " Am. Ind. Hyg. Assoc. J. **31**, 546 (1970).

14 T. Hatch and S. Choate, "Statistical Description of the Size Properties of Non-Uniform Particulate Substances," J. Franklin Inst. **207**, 369-387 (1929).

15. E. C. Hyatt, W. D. Moss, and H. F. Schulte, "Particle Size Studies on Uranium Aerosols from Machining and Metallurgy Operations," Am. Ind. Hyg. Assoc. J. **20**, 99-107 (1959).

16. H. E. Stokinger, "Toxicity Following Inhalation," in *Pharmacology and Toxicology of Uranium Compounds*, C. Voegtlin and H. C. Hodge, Eds., (McGraw-Hill, New York, 1949) Ch. 10, p. 501.

17. *Analytical Chemistry of the Manhattan Project*, C. J. Rodden, Ed. (McGraw-Hill, New York, 1950).